Research Square

Preprints are preliminary reports that have not undergone peer review.
They should not be considered conclusive, used to inform clinical practice,
or referenced by the media as validated information.

Mechanistic study of miR-124-3p targeting ATPase copper-transporting alpha to regulate copper homeostasis and cuproptosis sensitivity in hepatocellular carcinoma

Yanhua Ma

617747928@qq.com

First Clinical Medical College, Gansu University of Chinese Medicine https://orcid.org/0009-0000-2240-6413

Mingxia Lin

https://orcid.org/0009-0007-6451-2477

Yongjia Yang

Wei Yang

Article

Keywords: hepatocellular carcinoma, miR-124-3p, ATP7A, cuproptosis, copper homeostasis, non-coding RNA

Posted Date: September 24th, 2026

DOI: https://doi.org/10.21203/rs.3.rs-10859547/v1

License: This work is licensed under a Creative Commons Attribution 4.0 International License.
Read Full License

Additional Declarations: There is **NO** conflict of interest to disclose.

Abstract

Objective

This study aimed to investigate the role of microRNA-124-3p (miR-124-3p)-mediated regulation of ATPase copper-transporting alpha (ATP7A) in hepatocellular carcinoma (HCC) progression and cuproptosis sensitivity, providing new insights into copper metabolism-based therapeutic strategies.

Methods and Results

Bioinformatics analyses were performed to evaluate ATP7A expression, prognostic significance, and potential biological functions in HCC. ATP7A expression was significantly increased at both mRNA and protein levels in HCC tissues, and elevated ATP7A expression was associated with unfavorable overall survival. Further analysis identified miR-124-3p as a potential upstream regulator of ATP7A, which was confirmed by dual-luciferase reporter assays. qRT-PCR and Western blot analyses demonstrated reduced miR-124-3p expression and increased ATP7A expression in HCC cells. Functional assays revealed that miR-124-3p inhibition promoted HCC cell proliferation, migration, and invasion, whereas ATP7A silencing partially abolished these effects. Mechanistically, ATP7A knockdown increased intracellular copper accumulation, enhanced reactive oxygen species (ROS) production, promoted FDX1 and LIAS expression, and facilitated DLAT oligomerization, accompanied by G1-phase cell cycle arrest and apoptosis. Moreover, ATP7A depletion rescued the malignant phenotypes and cuproptosis-related alterations induced by miR-124-3p inhibition.

Conclusion

Our findings demonstrate that the miR-124-3p/ATP7A axis regulates copper homeostasis and cuproptosis sensitivity in HCC. Downregulation of miR-124-3p enhances ATP7A expression, promotes copper efflux, and reduces cuproptosis susceptibility, thereby facilitating HCC progression. Targeting this regulatory axis may represent a potential strategy for cuproptosis-based HCC therapy.

1. Introduction

Primary liver cancer is one of the most common malignant tumors worldwide and ranks as the third leading cause of cancer-related deaths[1].Among these, hepatocellular carcinoma (HCC) accounts for more than 80% of primary liver cancer cases and is the most common histological type[1].Because the clinical manifestations of HCC are subtle in the early stages and lack specific symptoms, most patients are already in the intermediate or advanced stages by the time they are diagnosed, which limits the opportunities for curative surgery[2].Although current therapeutic strategies have significantly improved the clinical management of HCC, their effectiveness remains constrained in advanced cases by intrinsic or acquired resistance and unsatisfactory long-term survival, highlighting the urgent need to identify novel molecular targets and therapeutic vulnerabilities[3].Therefore, further elucidation of the metabolic

dependence and cell death regulatory mechanisms underlying the onset and progression of HCC is of great significance for identifying new therapeutic targets and improving patient prognosis.

Copper is an indispensable micronutrient that participates in a broad range of biological processes, including mitochondrial respiration, oxidative stress regulation, iron metabolism, intracellular signaling, and the catalytic activity of copper-dependent enzymes.[4].However, intracellular levels of free copper must be strictly regulated; copper deficiency can impair the function of key enzymes, while excess copper can lead to protein toxicity, oxidative stress, and cellular damage. Cancer cells typically remodel their copper uptake, intracellular transport, storage, and efflux systems to meet their biological needs for rapid proliferation, angiogenesis, invasion, metastasis, and treatment resistance[5, 6],—thereby creating an abnormal state of copper metabolism that can be exploited by the tumor.

In 2022, Tsvetkov et al. systematically characterized for the first time a copper-dependent form of cell death distinct from apoptosis, necrosis, pyroptosis, and ferroptosis, and named it cuproptosis[7]. cuproptosis primarily occurs in cells that rely on mitochondrial oxidative phosphorylation. Excess copper can directly bind to acylated proteins in the citric acid cycle, promoting the abnormal aggregation of acylated proteins such as dihydrolipoamide acetyltransferase (DLAT), accompanied by the loss of Fe-S cluster proteins and protein toxic stress, ultimately inducing cell death[7]. Among these, ferredoxin 1 (FDX1) and lipoic acid synthetase (LIAS) are key molecules that regulate protein acylation and sensitivity to cuproptosis[7]. This finding suggests that tumor cells' dependence on copper homeostasis may represent a new metabolic vulnerability; modulating cellular copper homeostasis to enhance the sensitivity of tumor cells to cuproptosis may serve as a new therapeutic strategy[8].

ATPase copper-transporting alpha (ATP7A) is a copper-responsive P-type ATPase that serves as a key regulator of intracellular copper distribution. Under physiological copper conditions, ATP7A is predominantly retained in the trans-Golgi network, facilitating copper delivery to essential copper-dependent enzymes; when intracellular copper levels rise, ATP7A can translocate to the plasma membrane and the vesicular system, promoting the efflux of copper from the cell and thereby preventing excessive intracellular copper accumulation[4]. Therefore, abnormally high expression of ATP7A may maintain copper homeostasis in tumor cells by enhancing copper efflux, thereby reducing their sensitivity to copper toxicity and cuproptosis[7, 9]. Furthermore, previous studies have suggested that high ATP7A expression is associated with the malignant progression of various tumors and resistance to platinum-based drugs [10, 11]; in HCC patients, high ATP7A expression is also associated with poorer overall survival[12]. However, the upstream regulatory mechanisms and its role in cuproptosis in HCC remain to be fully elucidated.

MicroRNAs (miRNAs) constitute a major class of post-transcriptional gene regulators that modulate cellular phenotypes by controlling the expression of specific target genes. Through interaction with the 3'untranslated region (3'UTR) of target mRNAs, miRNAs regulate transcript stability and protein synthesis, contributing to the regulation of cancer progression, including tumor cell proliferation,

migration, and invasion, metabolic reprogramming, and cell death[13, 14]. miR-124-3p is considered a tumor-suppressor miRNA that is often downregulated in HCC tissues and cells. By targeting molecules such as ARRDC1, AKT2, and SIRT1, it inhibits hepatocellular carcinoma cell proliferation, epithelial-mesenchymal transition, and invasion and metastasis, and is involved in regulating sensitivity to sorafenib[15, 16].However, whether miR-124-3p participates in the regulation of copper homeostasis and cuproptosis in HCC through targeting copper transport-related molecules remains largely unexplored.

Based on this, this study first evaluated the expression patterns and clinical prognostic value of ATP7A in HCC using the TCGA, CPTAC, GEPIA 2, and survival analysis databases, and then predicted its potential biological functions by combining protein interaction networks with Gene Ontology (GO) and Kyoto Encyclopedia of Genes and Genomes (KEGG) enrichment analyses. Subsequently, candidate miRNAs upstream of ATP7A were identified through a combined screening using ENCORI[17]、miRDB[18]and TargetScan[19]and the direct targeting relationship between miR-124-3p and ATP7A was validated using a dual-luciferase reporter assay. Building on this foundation, we established cellular intervention and recovery models through miR-124-3p inhibition, overexpression, and ATP7A silencing. We systematically investigated the mechanisms by which the miR-124-3p/ATP7A axis regulates HCC malignant progression and copper-related phenotypes—including cell proliferation, migration, invasion, intracellular copper levels, oxidative stress, cell cycle, apoptosis, as well as FDX1, LIAS, and DLAT oligomerization, to systematically investigate the mechanisms by which the miR-124-3p/ATP7A axis regulates HCC malignant progression and cuproptosis-related phenotypes, with the aim of providing new experimental evidence for targeted therapies targeting copper metabolism in HCC.

2. Materials and Methods

2.1. Cell lines and cell culture

Normal human liver cells L02 (Cat. No.: TCH-C446), human hepatocellular carcinoma cells MHCC97H (Cat. No.: TCH-C258), Huh7 (Cat. No.: TCH-C217), and Hep3B (Cat. No.: TCH-C195) were all purchased from Suzhou Haixing Biotechnology Co., Ltd.; human hepatocellular carcinoma cells HepG2 were kindly provided by Professor Chen Qiqi.

HCC cell lines were maintained in high-glucose DMEM supplemented with 10% FBS and 1% penicillin–streptomycin, whereas L02 cells were grown in RPMI-1640 medium supplemented with the same additives. Cells were incubated under standard culture conditions (37°C, 5% CO_2), and subcultured upon reaching approximately 80–90% confluence.

2.2. Major reagents and antibodies

Fetal bovine serum (Cell-Box, Hong Kong, China), DMEM medium (Shangwei), miRNA-related reagents and qPCR kits (Accurate Biology, China), anti-ATP7A antibody (Abcam, UK), LIAS and DLAT antibodies (Immunoway, USA), PVDF membrane (Immobilon, USA), ECL chemiluminescent detection solution (Yisheng Biotechnology, China), transfection reagents and siRNA/mimics (Shengong Biotechnology,

China). A copper ion assay kit (Elabscience) and an ROS assay kit (Solarbio) were used for relevant functional assays.

2.3. Major instruments

Inverted fluorescence microscopes (ZEISS AxioVert 5; Olympus IX53), NanoDrop 2000c spectrophotometer (Thermo Fisher Scientific), CFX96 real-time quantitative PCR system (Bio-Rad), SpectraMax i3x microplate reader, flow cytometer (BriCyte E6, Mindray), etc.

2.4. Bioinformatics analysis

We used the GEPIA 2 and UALCAN databases to analyze differences in ATP7A expression between HCC and normal tissues; the UALCAN database further integrated TCGA and CPTAC data to assess its transcriptional and protein expression levels. The prognostic significance of ATP7A expression in HCC patients was evaluated using the Kaplan–Meier Plotter database, with overall survival (OS) serving as the clinical endpoint. Additionally, GO and KEGG pathway enrichment analyses were conducted based on ATP7A-associated gene sets to predict its potential biological functions and the signaling pathways in which it is involved.

2.5. Target gene prediction and dual-luciferase reporter assay

The binding site between miR-124-3p and ATP7A was predicted using a combination of the ENCORI[17] miRDB[18] and TargetScan[19]databases. The pmirGLO-ATP7A-WT and pmirGLO-ATP7A-MUT reporter plasmids were constructed.

Seed 293T cells into a 24-well plate (approximately 6 × 10^4 cells per well) and perform transfection when cell confluence reaches 50%–70%. The recombinant reporter plasmids were co-transfected with miR-124-3p mimics or corresponding negative controls using Lipofectamine 2000. Briefly, nucleic acids and plasmid DNA were separately prepared with the transfection reagent, followed by incubation to allow the formation of transfection complexes before being introduced into cultured cells.After 6 h of transfection, the transfection medium was replaced with fresh complete medium, and cells were maintained under standard culture conditions for an additional 48 h. Luciferase signals were measured using a dual-luciferase reporter assay system, and the activity of firefly luciferase was normalized to Renilla luciferase activity for relative quantification.

2.6. Cell Transfection

Seed MHCC97H cells in the logarithmic growth phase into a 6-well plate (2 × 10^5 cells per well). Mix miR-124-3p mimics, miR-124-3p inhibitor, ATP7A siRNA and the corresponding negative control were combined with the transfection reagent according to the manufacturer's protocol. The resulting nucleic acid–lipid complexes were prepared at room temperature and subsequently introduced into the cells.Replace the medium with fresh medium 6–8 hours after transfection. Collect cells at 48 and 72 hours post-transfection, respectively, for subsequent qRT-PCR and Western blot analysis.

2.7. Real-Time Quantitative PCR (qRT-PCR)

Total RNA was isolated using TRIzol reagent, and RNA quality was assessed by measuring concentration and purity. Subsequently, the extracted RNA was reverse-transcribed into cDNA for further quantitative analysis.Quantitative real-time PCR was performed using SYBR Green-based detection. GAPDH and U6 were selected as endogenous reference genes for normalization of mRNA and miRNA expression, respectively. Relative expression levels were determined using the comparative Ct (2^−ΔΔCt) method, and the primer information is provided in Table 1.

Table 1
List of qRT-PCR primers used

Gene name	Forward/reverse primer sequence (5'→3')	Amplicon size (bp)
hsa-miR-125b-5p (*Homo sapiens*)	TCCCTGAGACCCTAACTTGT TAAGGCACGCGGTGAATGC	76
RNU6 (U6) (*Homo sapiens*)	GGAACGATACAGAGAAGATTAGC TGGAACGCTTCACGAATTTGCG	94
ATP7A (*Homo sapiens*)	GACCAATGCCTATGCCATCC GCTGCTATTCCCACTGTCCC	132
GAPDH (*Homo sapiens*)	GATTCCACCCATGGCAAATTC CTGGAAGATGGTGATGGGATT	183

2.8. Western blot assay

After cell lysis to obtain total protein, protein concentration was determined using the BCA method, and sample loading volumes were standardized. Samples were treated differently depending on the assay objective: (1) non-boiling reducing conditions were used for ATP7A detection; (2) denaturation at 95°C was used for FDX1 and LIAS detection; (3) non-reducing, non-denaturing conditions were used for DLAT oligomer detection. Western blotting was performed to determine protein expression levels. Briefly, separated proteins were resolved by SDS-PAGE and electrotransferred onto PVDF membranes. After blocking, membranes were incubated with specific primary antibodies at 4°C overnight, followed by incubation with corresponding secondary antibodies at room temperature for 1 h. Protein signals were visualized using an ECL detection system, and densitometric analysis was conducted with ImageJ software. GAPDH or β-actin served as the loading control.

2.9. CCK-8 Cell Proliferation Assay

At 24 h following transfection, cells were redistributed into 96-well plates at a density of 2.5 × 10^3 cells per well. Cell viability was subsequently evaluated using the CCK-8 assay at indicated time points (0, 24,

48, 72, and 96 h) after reagent addition,and absorbance values were measured at a wavelength of 450 nm.

2.10. Cell scratch assay

Scratch assays were performed 36 hours after transfection, when cell confluence reached 90% or higher. After creating scratches with a sterile pipette tip, the medium was replaced with low-serum medium, and photographs were taken at 0, 24, and 48 hours to document the results. The scratch healing rate was calculated using ImageJ.

2.11. Transwell migration and invasion assays

For migration assays, the substrate was left uncoated; for invasion assays, the substrate was pre-coated with matrix gel. Cell suspensions were loaded into the upper compartment of the Transwell inserts, while the lower wells were filled with medium supplemented with 20% FBS to establish a chemoattractant gradient. After 48 h (migration) or 60 h (invasion) of culture, the cells were fixed, stained, and the number of cells that had traversed the membrane was counted.

2.12. Detection of intracellular copper ions

48 hours after transfection, the intracellular copper ion concentration was measured using a colorimetric assay kit. The results were normalized for protein concentration and calculated based on a standard curve.

2.13. Measurement of reactive oxygen species (ROS) levels

Cells were labeled with the DCFH-DA probe, incubated at 37°C, washed. Following probe loading, cells were subjected to flow cytometric analysis, and ROS accumulation was quantified based on the fluorescence intensity detected at an excitation wavelength of 488 nm and an emission wavelength of 525 nm.

2.14 Apoptosis and cell cycle analysis

Cell apoptosis was detected using the Annexin V-FITC/PI double-staining method. For cell cycle analysis, cells were fixed in 70% ethanol and stained with propidium iodide (PI). The DNA content distribution was subsequently evaluated by flow cytometry to determine the proportion of cells in different cell cycle phases.

2.15. Statistical analysis

All experiments were repeated ≥ 3 times, and data are presented as mean ± standard deviation. Comparisons between two groups were performed using an independent-samples t-test; comparisons among multiple groups were performed using one-way analysis of variance (ANOVA); and comparisons between groups were performed using the LSD or Tukey test. A P-value < 0.05 was considered statistically significant. Data analysis was performed using GraphPad Prism 10.1.2 software.

3. Results

3.1. Analysis of abnormal expression of ATP7A in HCC tissue and its prognostic value

To characterize the dysregulation of ATP7A in HCC and explore its potential clinical relevance,a comprehensive analysis was conducted using multiple public databases. Analysis using the GEPIA 2 platform revealed that ATP7A mRNA expression was markedly elevated in HCC tissues compared with normal liver tissues (Fig. 1A). Analysis of the TCGA database was consistent with these findings, further confirming the high expression of ATP7A in HCC (Fig. 1B, $P < 0.0001$). At the protein level, analysis of the CPTAC database showed that ATP7A expression was also significantly elevated in HCC tissues (Fig. 1C, $P < 0.01$). Survival analysis results indicated that, based on the GEPIA 2 database, Patients exhibiting elevated ATP7A expression displayed a poorer overall survival (OS) outcome compared with those with lower ATP7A levels (Fig. 1D, $P < 0.05$) ; the Kaplan–Meier Plotter database analysis yielded consistent results (Fig. 1E, $P < 0.01$), indicating that elevated ATP7A expression may serve as an unfavorable prognostic indicator in HCC patients. In summary, ATP7A is upregulated in HCC at both the transcriptional and protein levels, and elevated expression levels were indicative of unfavorable survival outcomes in patients.

Figure 1 Bioinformatics analysis of ATP7A expression and its prognostic significance in hepatocellular carcinoma

(A) Comparison of ATP7A expression levels between hepatocellular carcinoma (LIHC) tissues and normal liver tissues in the GEPIA 2 dataset; (B) Analysis of ATP7A mRNA expression differences based on TCGA transcriptomic data; (C) Analysis of ATP7A protein expression differences based on CPTAC proteomic data; (D) Kaplan–Meier survival analysis of OS based on the GEPIA 2 database, comparing high and low ATP7A expression groups; (E) Survival analysis based on the Kaplan–Meier Plotter database evaluating the association between ATP7A expression and prognosis in patients with hepatocellular carcinoma.

3.2. Functional enrichment analysis of ATP7A-related genes

To investigate the potential biological functions of ATP7A and its associated regulatory pathways, this study first constructed a protein interaction network for ATP7A based on the STRING database. The results showed that ATP7A has potential interactions with various proteins, forming a relatively dense interaction network (Fig. 2A). Building on this, a functional enrichment analysis was performed on the genes interacting with ATP7A. GO-based functional enrichment analysis suggested that ATP7A-associated genes were closely linked to biological processes involved in metal ion handling, copper metabolism, and redox homeostasis (Fig. 2C); KEGG pathway analysis suggested that ATP7A-related genes were closely linked to copper homeostasis-associated pathways, including copper transport and

metabolic regulation (Fig. 2B). In summary, ATP7A and its interaction network may play an important role in biological processes related to copper metabolism, providing a bioinformatics basis for further research into the role of ATP7A in the regulation of copper metabolism in HCC.

Figure 2. Bioinformatic analysis reveals the potential involvement of ATP7A in copper metabolism-related biological processes

(A) Protein-protein interaction (PPI) network analysis of ATP7A and its interacting proteins based on the STRING database. (B-C) Bioinformatic annotation of ATP7A-associated genes using GO classification (C) and KEGG pathway enrichment analysis (B),revealing the potential biological processes and signaling pathways involved in ATP7A regulation.

3.3. Validation of miR-124-3p as a direct target of ATP7A

To identify potential upstream miRNAs that regulate ATP7A expression, this study conducted a target prediction analysis using the ENCORI[17],miRDB[18] and TargetScan[19]databases. The results of the intersection analysis indicated that miR-124-3p and miR-223-3p may have potential binding relationships with ATP7A (Fig. 3A and 3B). Based on previous reports and their potential regulatory roles in HCC, this study further selected miR-124-3p as a candidate miRNA for subsequent validation. TargetScan prediction results showed that miR-124-3p possesses a conserved complementary binding site in the 3'-UTR region of ATP7A mRNA (Fig. 3C). To further validate the direct targeting relationship between the two, dual-luciferase reporter vectors containing both the wild-type (WT) and mutant (MUT) sequences of the ATP7A 3'-UTR were constructed and co-transfected with miR-124-3p mimics or NC mimics. Luciferase reporter assays demonstrated that miR-124-3p overexpression significantly decreased the activity of the ATP7A-WT reporter construct compared with the NC mimics group, whereas no significant effect was detected on the ATP7A-MUT reporter, while having no apparent effect on the luciferase activity of the ATP7A-MUT vector (Fig. 3D). These results indicate that miR-124-3p specifically binds to the 3'-UTR region of ATP7A mRNA, suggesting that ATP7A may be a direct target gene of miR-124-3p.

Figure 3. Bioinformatic prediction and experimental validation of the targeting relationship between miR-124-3p and ATP7A

(A) Candidate miRNAs targeting ATP7A were screened using three databases (ENCORI, miRDB, and TargetScan). (B) Summary of prediction scores for candidate miRNAs across the three databases. (C) Predicted binding site and seed sequence pairing between miR-124-3p and the 3'-UTR of ATP7A based on TargetScan analysis. (D) Dual-luciferase reporter assay identifying ATP7A as a direct target of miR-124-3p. Note: NS, not significant; $^{**}P < 0.01$.

3.4. Expression profiles of miR-124-3p and ATP7A in HCC cells

To clarify the expression patterns of miR-124-3p and ATP7A in HCC cells, this study used normal liver cells (L02) as a control to detect the baseline expression levels of both in MHCC97H, Huh7, Hep3B, and

HepG2 cells. qRT-PCR results showed that, compared with L02 cells, miR-124-3p expression levels were significantly reduced in all four HCC cell lines (Fig. 4B), while ATP7A mRNA expression levels exhibited a marked upward trend (Fig. 4A). Further analysis of ATP7A protein expression via Western blot revealed that ATP7A protein levels were significantly higher in HCC cell lines than in L02 cells (Fig. 4C and D). A comprehensive analysis of the expression profiles across the cell lines revealed that MHCC97H cells exhibited lower miR-124-3p expression and higher ATP7A expression; therefore, MHCC97H cells were selected as the model for subsequent functional validation and mechanistic studies.

Figure 4. Expression patterns of miR-124-3p and ATP7A in normal hepatocytes and hepatocellular carcinoma cell lines

(A) qRT-PCR analysis of ATP7A mRNA expression in normal hepatocytes (L02) and hepatocellular carcinoma (HCC) cell lines. (B) qRT-PCR analysis of miR-124-3p expression in the indicated cell lines. (C) Representative immunoblotting images showing ATP7A protein levels in normal hepatocytes and HCC cell lines. (D) Relative ATP7A protein abundance was quantified by grayscale analysis.**Note: All statistical comparisons were performed relative to the L02 cell group. ***$P < 0.001$, ****$P<0.0001$.

3.5. miR-124-3p downregulates ATP7A expression in MHCC97H cells

To further validate the regulatory role of miR-124-3p on ATP7A expression, this study established miR-124-3p overexpression and knockdown models in MHCC97H cells. qRT-PCR results showed that, compared with the corresponding negative control groups, the expression level of miR-124-3p in the cells was significantly reduced following transfection with the miR-124-3p inhibitor; conversely, the expression level of miR-124-3p was markedly increased following transfection with miR-124-3p mimics, indicating that the miR-124-3p intervention models were successfully established (Fig. 5A, B). Further analysis of changes in ATP7A expression revealed that inhibiting miR-124-3p expression significantly promoted ATP7A mRNA expression, whereas overexpression of miR-124-3p markedly reduced ATP7A mRNA levels (Fig. 5C). Western blot results showed that changes in ATP7A protein expression were consistent with those at the mRNA level: miR-124-3p knockdown significantly enhanced ATP7A protein expression, whereas miR-124-3p overexpression markedly inhibited ATP7A protein accumulation (Fig. 5D, E). In summary, the results of the cellular functional validation indicate that miR-124-3p negatively regulates ATP7A expression at both the mRNA and protein levels, further confirming the existence of a stable negative regulatory relationship between miR-124-3p and ATP7A.

Figure 5. Validation of miR-124-3p-mediated negative regulation of ATP7A expression in MHCC97H cells

(A) Validation of miR-124-3p knockdown efficiency in MHCC97H cells by qRT-PCR. (B) Confirmation of miR-124-3p overexpression in MHCC97H cells using qRT-PCR.(C) qRT-PCR analysis of ATP7A mRNA expression in MHCC97H cells following different treatments. (D) Western blot analysis of ATP7A protein expression in MHCC97H cells. (E) Densitometric quantification of ATP7A protein expression. **Note: Untreated, untreated group; NC, negative control; miR-mimics, miR-124-3p mimics; miR-inh, miR-124-3p

inhibitor. All statistical comparisons were performed relative to the Untreated group. NS, not significant; $^{**}P < 0.01$, $^{***}P < 0.001$, $^{****}P < 0.0001$.

3.6. miR-124-3p targets ATP7A to regulate proliferation, migration, and invasion in MHCC97H cells

To elucidate the regulatory relationship between miR-124-3p and ATP7A in HCC progression, rescue experiments were conducted by combining miR-124-3p inhibition with ATP7A knockdown. Four groups—inh-NC + si-NC, inh-NC + si-ATP7A, miR-inh + si-NC, and miR-inh + si-ATP7A—were set up for functional validation. CCK-8 assay results showed that, compared with the control group, inhibition of miR-124-3p expression significantly enhanced the proliferative activity of MHCC97H cells, whereas silencing ATP7A alone markedly inhibited cell proliferation (Fig. 6A). Further analysis revealed that simultaneous interference with ATP7A expression against the background of miR-124-3p knockdown significantly attenuated the proliferation-enhancing effect induced by miR-124-3p deficiency. Results from the cell scratch assay showed that cell migration capacity was significantly enhanced following miR-124-3p inhibition, as evidenced by accelerated scratch healing; whereas ATP7A silencing reduced cell migration levels and partially reversed the migration-promoting effect caused by miR-124-3p inhibition (Fig. 6B, C). Further assessment of cell migration and invasion capabilities via Transwell assays revealed that miR-124-3p inhibition significantly increased the number of cells crossing the membrane, whereas ATP7A knockdown markedly reduced both cell migration and invasion capabilities (Fig. 6D, E). Combining ATP7A silencing with miR-124-3p inhibition also partially restored the cell migration and invasion phenotypes. In summary, functional recovery experiments indicate that miR-124-3p influences HCC cell proliferation, migration, and invasion by regulating ATP7A expression, and that ATP7A is one of the key downstream molecules mediating the tumor-suppressive effects of miR-124-3p.

Figure 6. miR-124-3p regulates the proliferation, migration, and invasion of MHCC97H cells by targeting ATP7A

(A) Cell proliferation activity of MHCC97H cells in the indicated groups was assessed by CCK-8 assay at 0, 24, 48, 72, and 96 h after transfection. (B) Representative images of wound healing assays showing the migratory ability of MHCC97H cells at 0, 24, and 48 h. (C) Quantitative analysis of wound closure rates in the indicated groups. (D) Representative crystal violet staining images of Transwell assays evaluating cell migration and invasion abilities. (E) Quantification of migrated and invaded cells in Transwell assays. Note: si-NC, small interfering RNA negative control; si-ATP7A, ATP7A-specific small interfering RNA. $^{*}P < 0.05$, $^{**}P < 0.01$, $^{***}P < 0.001$, $^{****}P < 0.0001$

3.7. The miR-124-3p/ATP7A axis regulates molecular features associated with cuproptosis in HCC cells

To further elucidate the effect of the miR-124-3p/ATP7A regulatory axis on the sensitivity of HCC cells to cuproptosis, this study further examined changes in key molecular events associated with cuproptosis. First, the efficiency of ATP7A siRNA interference was validated. Transfection efficiency was assessed

using FAM-labeled fragments; the results showed that exogenous nucleic acids could be effectively delivered into MHCC97H cells, providing a foundation for subsequent intervention experiments (Fig. 7A). Subsequently, effective siRNA sequences for ATP7A were screened by transfecting different ATP7A siRNA sequences. qRT-PCR and Western blot results showed that both si-ATP7A-1 and si-ATP7A-2 significantly reduced ATP7A mRNA and protein expression levels; among them, si-ATP7A-2 exhibited higher silencing efficiency and was therefore selected for subsequent experiments (Fig. 7B–D). Building on this, we utilized the four recovery experimental systems established earlier (inh-NC + si-NC, inh-NC + si-ATP7A, miR-inh + si-NC, and miR-inh + si-ATP7A) to further analyze the effects of the miR-124-3p/ATP7A axis on molecules associated with cuproptosis. qRT-PCR results showed that inhibiting miR-124-3p expression significantly increased ATP7A mRNA levels, whereas this change was markedly reversed upon combined silencing of ATP7A (Fig. 7E). Cuproptosis depends on abnormal interactions between copper ions and acylated proteins associated with the mitochondrial tricarboxylic acid cycle, in which the oligomerization of FDX1, LIAS, and DLAT is considered a key molecular event involved in this process[7]. Western blot analysis further demonstrated that miR-124-3p inhibition promotes ATP7A protein expression and reduces the expression levels of the cuproptosis-associated proteins FDX1 and LIAS; in contrast, ATP7A silencing reduces ATP7A protein levels while promoting FDX1 and LIAS expression (Fig. 7F–I). Results from non-reducing Western blot analysis showed that DLAT oligomerization signals were weak in the control and miR-124-3p inhibition groups, whereas DLAT oligomerization levels were significantly enhanced following ATP7A silencing; co-knockdown of ATP7A against the background of miR-124-3p inhibition also restored DLAT oligomerization levels (Fig. 7F). These results indicate that the miR-124-3p/ATP7A axis can influence the molecular characteristics associated with cuproptosis in HCC cells, and that ATP7A may participate in the regulation of cuproptosis sensitivity in HCC cells by modulating intracellular copper homeostasis.

Figure 7. The miR-124-3p/ATP7A axis regulates cuproptosis-associated molecular changes in HCC cells

(A) Visualization of intracellular FAM fluorescence in MHCC97H cells following oligonucleotide transfection.(B) qRT-PCR analysis of ATP7A mRNA expression in MHCC97H cells transfected with different ATP7A siRNAs for screening effective knockdown sequences. (C) Western blot analysis of ATP7A protein expression after ATP7A silencing. (D) Densitometric quantification of ATP7A protein expression. (E) qRT-PCR analysis of ATP7A mRNA expression in the four rescue groups. (F) Western blot analysis of ATP7A, FDX1, and LIAS expression, together with DLAT oligomerization under non-reducing conditions, in the indicated groups. (G-I) Quantitative analysis of ATP7A, FDX1, and LIAS protein expression based on densitometric measurements. **Note: NS, not significant; ***P*<0.01, ****P*<0.001, *****P*<0.0001.

3.8. The miR-124-3p/ATP7A axis regulates copper homeostasis, oxidative stress, and apoptosis-related phenotypes in HCC cells

To further investigate the effects of the miR-124-3p/ATP7A axis on copper homeostasis and cell fate in HCC cells, this study measured intracellular Cu^{2+} levels, ROS levels, cell cycle distribution, and apoptosis in MHCC97H cells under various treatment conditions. First, changes in intracellular Cu^{2+} levels were measured using a microplate reader. The results showed that, compared with the control group, silencing ATP7A significantly increased intracellular Cu^{2+} levels in MHCC97H cells, whereas inhibiting miR-124-3p expression reduced the accumulation of intracellular copper ions; following combined silencing of ATP7A against a background of miR-124-3p knockdown, intracellular Cu^{2+} levels were significantly restored to elevated levels (Fig. 8D). These results suggest that the miR-124-3p/ATP7A axis influences intracellular copper homeostasis by regulating ATP7A-mediated copper transport. Since excess copper can induce oxidative stress and protein toxic stress, this study further employed the DCFH-DA fluorescent probe combined with flow cytometry to detect intracellular ROS levels. The results showed that ATP7A silencing significantly enhanced cellular ROS fluorescence signals, suggesting that disruption of copper homeostasis may be accompanied by increased oxidative stress[20]; in contrast, ROS levels were reduced in the miR-124-3p inhibition group; and co-knockdown of ATP7A partially reversed the decrease in ROS levels caused by miR-124-3p inhibition (Fig. 8A, E). Cell cycle analysis results showed that, compared with the control group, the proportion of MHCC97H cells in the G1 phase increased significantly after ATP7A silencing, while the proportion of cells in the G2/M phase decreased significantly, suggesting that ATP7A knockdown leads to inhibition of cell cycle progression. In contrast, the miR-124-3p inhibition group exhibited a trend toward a decreased G1 phase proportion and an increased G2/M phase proportion, suggesting that low miR-124-3p expression may promote tumor cell cycle progression; combined silencing of ATP7A against the background of miR-124-3p knockdown partially reversed these cell cycle changes (Fig. 8B, F). Flow cytometric analysis using Annexin V-FITC/PI double staining revealed that ATP7A silencing significantly increased the overall apoptosis rate in MHCC97H cells, with a particularly marked increase in the proportion of cells in late apoptosis; in contrast, miR-124-3p inhibition reduced apoptosis levels. Following co-knockdown of ATP7A, the reduced apoptosis phenotype induced by miR-124-3p inhibition was markedly reversed (Fig. 8C, G). In summary, the results of functional phenotypic analysis indicate that the miR-124-3p/ATP7A axis influences the response of HCC cells to cuproptosis by regulating intracellular copper homeostasis, thereby altering oxidative stress levels, cell cycle progression, and cell survival status. Abnormally elevated ATP7A levels may promote HCC cell survival by limiting intracellular copper accumulation, reducing oxidative stress, and decreasing sensitivity to cell death.

Figure 8. The miR-124-3p/ATP7A axis influences cuproptosis-related phenotypes in HCC cells by regulating copper homeostasis

(A) Representative flow cytometry profiles showing intracellular ROS levels in MHCC97H cells from the indicated groups. (B) Representative flow cytometry profiles showing cell cycle distribution in MHCC97H cells. (C) Representative Annexin V-FITC/PI staining profiles showing apoptosis in MHCC97H cells. (D) Measurement of intracellular Cu^{2+} levels in MHCC97H cells from the indicated groups. (E) Quantitative analysis of intracellular ROS levels based on mean fluorescence intensity (MFI). (F) Quantitative analysis of cell cycle distribution among G1, S, and G2/M phases. (G) Quantitative analysis of total apoptosis

rates. **Note: Intracellular ROS levels were detected using the DCFH-DA probe by flow cytometry. Data are presented as mean ± SD from three independent experiments. **P<0.01, ***P<0.001, ****P<0.0001.

4. Discussion

The onset and progression of HCC depend not only on abnormalities in classical genetic and signaling pathways but are also accompanied by significant metabolic remodeling. In recent years, the unique metabolic characteristics of tumor cells have increasingly become a key focus in the search for novel therapeutic strategies. Copper, as an essential trace element for maintaining cellular life, plays a critical role in redox regulation, mitochondrial respiration, and the maintenance of enzyme activity[4]. However, abnormal copper metabolic homeostasis can also promote the adaptive survival of tumor cells and create potential metabolic vulnerabilities[6]. This study found that HCC cells downregulate miR-124-3p to lift its negative regulation of ATP7A, leading to abnormally elevated ATP7A levels, which enhance copper efflux and reduce cellular sensitivity to cuproptosis stimuli, thereby promoting the maintenance of the malignant tumor phenotype. Further studies indicate that targeting ATP7A can reactivate cuproptosis-related molecular events, suggesting that the miR-124-3p/ATP7A axis may serve as a key regulatory network linking non-coding RNA regulation, copper homeostasis imbalance, and HCC progression.

Copper homeostasis disruption has been recognized as a key component of tumor metabolic reprogramming. Under normal conditions, cells maintain a dynamic equilibrium of copper ion levels through systems for copper uptake, transport, storage, and excretion[21]; however, due to their rapid proliferation and high metabolic demands, tumor cells often need to reorganize their copper metabolic networks to meet their survival needs, such as rapid proliferation and energy metabolism[4, 22]. Previous studies have shown that abnormalities in copper metabolism are present in HCC tissues, accompanied by altered expression of various copper transport-related genes and cuproptosis regulatory molecules[23, 24], suggesting that the remodeling of copper homeostasis may be involved in key processes of HCC development and progression. ATP7A, a key copper transporter involved in maintaining cellular copper homeostasis, is primarily responsible under normal physiological conditions for the intracellular distribution of copper ions and the efflux of excess copper to prevent copper-induced toxicity. In the tumor microenvironment, however, enhanced copper efflux may serve as a key strategy for cancer cells to adapt to high metabolic demands and avoid copper-induced toxicity[23, 25]. Based on an analysis of multiple public databases, this study found that ATP7A is significantly overexpressed in HCC tissues and is associated with poorer survival outcomes in patients, further suggesting that ATP7A may be involved in the metabolic adaptation and malignant progression of HCC cells. Consistent with the findings of this study, previous research has reported that abnormal ATP7A expression is closely associated with the development and progression of various solid tumors, including HCC, gastric cancer, and breast cancer, and may be involved in tumor cell invasion, drug resistance, and the regulation of immunotherapy[10, 12, 26, 27]. In recent years, with the introduction of the concept of cuproptosis, the functional significance of ATP7A in tumors has been further expanded. Zhao et al. found that in KRAS-mutant lung adenocarcinoma, tumor cells are highly dependent on copper homeostasis for survival, and inhibiting

ATP7A-mediated copper efflux increases intracellular copper accumulation and enhances the cells' sensitivity to cuproptosis-inducing stimuli[28]. Zhao et al. demonstrated that ginsenoside Rh1 enhances copper accumulation and cuproptosis in gastric cancer cells by downregulating ATP7A, thereby attenuating cuproptosis-associated immune evasion[29]. It suggests that ATP7A is not only an important transporter for maintaining cellular copper homeostasis but may also serve as a key adaptive factor enabling tumor cells to evade cuproptosis. By enhancing copper efflux, ATP7A reduces intracellular copper accumulation and associated protein toxic stress, thereby attenuating the sensitivity of HCC cells to cuproptosis and promoting tumor cell survival. Therefore, targeting ATP7A or regulating its upstream molecular network may enhance the response of HCC cells to cuproptosis-inducing strategies, providing a new research direction for the development of precision therapies based on copper metabolic vulnerabilities.

As important post-transcriptional regulatory factors, miRNAs play a wide range of roles in tumorigenesis, tumor progression, and metabolic adaptation[13]. Previous studies have shown that non-coding RNAs can participate in the remodeling of copper homeostasis in tumors by regulating copper transporters. For example, Zhang et al. found that in oral squamous cell carcinoma, exosome-derived miRNAs can influence copper homeostasis and promote tumor progression by regulating ATP7A[11]; furthermore, miR-133a-5p has been reported to promote cuproptosis in HCC cells by regulating ATP7B[30]. The above studies suggest that copper transporters may serve as key regulatory nodes linking tumor microenvironment signaling, non-coding RNA regulation, and cell death pathways. In recent years, miR-124-3p has been recognized as a tumor-suppressing miRNA; it is downregulated in various malignant tumors and can influence cell proliferation, migration, invasion, and treatment sensitivity by regulating multiple target genes. In HCC, previous studies have shown that miR-124-3p can inhibit tumor progression by targeting molecules such as CRKL and SIRT1[31, 32]; however, there remains a lack of research on whether it is involved in the regulation of copper metabolism and the process of cuproptosis. Through a combination of bioinformatics predictions and dual-luciferase reporter assays, this study demonstrated for the first time that ATP7A is a direct target gene of miR-124-3p, revealing a new function of miR-124-3p in regulating copper metabolism in HCC cells. This finding expands the spectrum of biological functions of miR-124-3p and suggests that non-coding RNAs may influence the mode of tumor cell death by regulating metal ion homeostasis.

From the perspective of functional regulation, the miR-124-3p/ATP7A axis not only influences changes in molecules associated with cuproptosis but also participates in regulating the malignant biological behavior of HCC cells. It is worth noting that cuproptosis differs significantly from apoptosis in the traditional sense; its initiating events do not depend on the typical caspase cascade[33, 34], but rather primarily result from mitochondrial metabolic dysfunction and protein toxic stress[7, 35]. Therefore, the increased cell cycle arrest and late-stage cell death phenotypes observed in this study during cuproptosis induction may reflect the combined effects of the collapse of cellular energy metabolism and impaired membrane integrity following the disruption of copper homeostasis. This suggests that

cuproptosis is not only an independent form of cell death but may also further influence proliferative capacity and survival advantage by altering the metabolic state of tumor cells.

This study validated, through multi-level experiments, the role of the miR-124-3p/ATP7A axis in regulating HCC sensitivity to cuproptosis and tumor malignant phenotypes, providing potential targets for cuproptosis-based HCC treatment strategies. However, certain limitations remain: First, the study was primarily based on in vitro cellular models, and its biological significance requires further validation through animal experiments and clinical samples; Second, the specific molecular network through which ATP7A regulates cuproptosis remains unclear, and in particular, its relationship with mitochondrial metabolism and protein toxic stress requires further investigation. Future studies could further elucidate the role of this regulatory axis in tumor heterogeneity and treatment resistance. At the same time, restoring miR-124-3p expression or specifically inhibiting ATP7A function using a miRNA delivery system may serve as a potential therapeutic strategy to enhance HCC sensitivity to cuproptosis.

Figure 9. Proposed model illustrating the role of the miR-124-3p/ATP7A axis in regulating copper homeostasis and cuproptosis sensitivity in hepatocellular carcinoma.

Downregulation of miR-124-3p in HCC cells alleviates post-transcriptional repression of ATP7A by binding to the 3'UTR of ATP7A mRNA, leading to increased ATP7A expression and enhanced copper efflux. Elevated ATP7A maintains intracellular copper homeostasis and decreases cuproptosis susceptibility, thereby promoting HCC progression. Conversely, ATP7A silencing induces intracellular Cu^{2+} accumulation and activates cuproptosis-related responses, resulting in inhibition of malignant phenotypes in HCC cells.

5. Conclusion

This study confirms that low expression of miR-124-3p in HCC promotes ATP7A-mediated copper ion efflux by lifting the inhibition on ATP7A, thereby reducing the sensitivity of tumor cells to cuproptosis and promoting the malignant progression of HCC. The study reveals a new mechanism by which the miR-124-3p/ATP7A axis regulates copper homeostasis and cuproptosis, providing a new theoretical basis for targeted therapy of cuproptosis in HCC.

CRediT authorship contribution statement

Mingxia Lin: Conceptualization, Methodology, Investigation, Formal analysis, Data curation, and Writing – original draft. Yongjia Yang: Validation, Investigation, and Data curation. Wei Yang: Methodology, Investigation, and Writing – original draft. Yanhua Ma: Methodology, Investigation, and Funding acquisition.

Declarations

CRediT authorship contribution statement

Mingxia Lin: Conceptualization, Methodology, Investigation, Formal analysis, Data curation, and Writing – original draft. Yongjia Yang: Validation, Investigation, and Data curation. Wei Yang: Methodology, Investigation, and Writing – original draft. Yanhua Ma: Methodology, Investigation, and Funding acquisition.

Funding

This work was supported by the General Project of the Gansu Province Joint Scientific Research Fund (Grant No. 23JRRA1523), the Graduate Student Innovation and Entrepreneurship Fund of Gansu University of Chinese Medicine (Grant No. 2026CXCY-047), and the 2025 Gansu Provincial Traditional Chinese Medicine Research Project (Grant No. GZKG-2025-90).

Declaration of competing interest

The authors declare that they have no known competing financial interests or personal relationships that could have appeared to influence the work reported in this paper.

Declaration of AI-Assisted Writing

During the preparation of this manuscript, the authors used Chat GPT 5.5 for language polishing and to improve the clarity and readability of the manuscript. The authors subsequently reviewed and edited all AI-assisted content as appropriate and assume full responsibility for the content, accuracy, and integrity of the published article.

Acknowledgments

We sincerely acknowledge the Experimental Center of Clinical Medicine, The First Clinical Medical School, Gansu University of Chinese Medicine, for providing the laboratory facilities and technical support for this study. We are also grateful to Professor Yong An for his valuable guidance on the feasibility, study design, and research direction.

References

1. SINGAL A G, KANWAL F, LLOVET J M. Global trends in hepatocellular carcinoma epidemiology: implications for screening, prevention and therapy [J]. Nat Rev Clin Oncol, 2023, 20(12): 864–84.
2. LI R, WANG Y, ZHANG X, et al. Exosome-mediated secretion of LOXL4 promotes hepatocellular carcinoma cell invasion and metastasis [J]. Mol Cancer, 2019, 18(1): 18.
3. VOGEL A, MEYER T, SAPISOCHIN G, et al. Hepatocellular carcinoma [J]. Lancet, 2022, 400(10360): 1345–62.
4. LUTSENKO S, ROY S, TSVETKOV P. Mammalian copper homeostasis: physiological roles and molecular mechanisms [J]. Physiol Rev, 2025, 105(1): 441–91.

5. SHAN D, SONG J, REN Y, et al. Copper in cancer: friend or foe? Metabolism, dysregulation, and therapeutic opportunities [J]. Cancer Commun (Lond), 2025, 45(5): 577–607.
6. GE E J, BUSH A I, CASINI A, et al. Connecting copper and cancer: from transition metal signalling to metalloplasia [J]. Nat Rev Cancer, 2022, 22(2): 102–13.
7. TSVETKOV P, COY S, PETROVA B, et al. Copper induces cell death by targeting lipoylated TCA cycle proteins [J]. Science, 2022, 375(6586): 1254–61.
8. TANG D, KROEMER G, KANG R. Targeting cuproplasia and cuproptosis in cancer [J]. Nat Rev Clin Oncol, 2024, 21(5): 370–88.
9. [illegible], [illegible], [illegible], et al. ATP[illegible]α[illegible] [J]. [illegible](), 2026, 64(4): 117–24.
10. SHA S, SI L, WU X, et al. Prognostic analysis of cuproptosis-related gene in triple-negative breast cancer [J]. Front Immunol, 2022, 13: 922780.
11. ZHANG S, LIU X, ZHANG J, et al. Cancer-associated fibroblasts promote oral squamous cell carcinoma progression by targeting ATP7A via exosome-mediated paracrine miR-148b-3p [J]. Cell Signal, 2025, 128: 111631.
12. SHAO K, SHEN H, CHEN X, et al. Copper transporter gene ATP7A: A predictive biomarker for immunotherapy and targeted therapy in hepatocellular carcinoma [J]. Int Immunopharmacol, 2023, 114: 109518.
13. DI LEVA G, GAROFALO M, CROCE C M. MicroRNAs in cancer [J]. Annu Rev Pathol, 2014, 9: 287–314.
14. GARZON R, MARCUCCI G, CROCE C M. Targeting microRNAs in cancer: rationale, strategies and challenges [J]. Nat Rev Drug Discov, 2010, 9(10): 775–89.
15. DONG Z B, WU H M, HE Y C, et al. MiRNA-124-3p.1 sensitizes hepatocellular carcinoma cells to sorafenib by regulating FOXO3a by targeting AKT2 and SIRT1 [J]. Cell Death Dis, 2022, 13(1): 35.
16. ZHAO Q, JIANG F, ZHUANG H, et al. MicroRNA miR-124-3p suppresses proliferation and epithelial-mesenchymal transition of hepatocellular carcinoma via ARRDC1 (arrestin domain containing 1) [J]. Bioengineered, 2022, 13(4): 8255–65.
17. ZHOU K, HUANG J, LIU S, et al. An encyclopedic regulatory and functional atlas of RNA interactomes [J]. Nat Methods, 2026, 23(6): 1109–14.
18. CHEN Y, WANG X. miRDB: an online database for prediction of functional microRNA targets [J]. Nucleic Acids Res, 2020, 48(D1): D127-d31.
19. AGARWAL V, BELL G W, NAM J W, et al. Predicting effective microRNA target sites in mammalian mRNAs [J]. Elife, 2015, 4.
20. TAO X, WANG H, WANG Q, et al. Marine Natural Product Chagosendine C Induces Cuproptosis in Colorectal Cancer Cells by Targeting FDX1 [J]. J Am Chem Soc, 2025, 147(41): 37089–103.
21. NIU L, SU W, JU L, et al. Innovative cross-intervention: copper ions and metabolic pathways in cancer therapy [J]. Cancer Biol Med, 2026, 23(1): 30–41.
22. YANG S, SONG Y, HU Y, et al. Multifaceted Roles of Copper Ions in Anticancer Nanomedicine [J]. Adv Healthc Mater, 2023, 12(23): e2300410.

23. WU Z, LV G, XING F, et al. Copper in hepatocellular carcinoma: A double-edged sword with therapeutic potentials [J]. Cancer Lett, 2023, 571: 216348.
24. ZHAO X, CHEN J, YIN S, et al. The expression of cuproptosis-related genes in hepatocellular carcinoma and their relationships with prognosis [J]. Front Oncol, 2022, 12: 992468.
25. DAS A, ASH D, FOUDA A Y, et al. Cysteine oxidation of copper transporter CTR1 drives VEGFR2 signalling and angiogenesis [J]. Nat Cell Biol, 2022, 24(1): 35–50.
26. PAN S, WU Q, LIU H, et al. ATP7A-mediated copper ion efflux reprogrammes tumour immunity and promotes cisplatin resistance in cervical cancer [J]. Cell Death Dis, 2026.
27. SHI Z, MAO Z, CUI M, et al. ATP7A as a prognostic biomarker and potential therapeutic target in gastric cancer [J]. Am J Transl Res, 2025, 17(1): 512–27.
28. ZHAO J, ZHANG W, ZENG Y, et al. Targeting ATP7A-Dependent Copper Metabolic Homeostasis Induces Cuproptosis and Suppresses the Progression of Mutant KRAS-Driven Lung Cancer [J]. Cancer Res, 2025, 85(20): 3999–4017.
29. ZHAO D, YUAN Q, WANG H, et al. Ginsenoside Rh1 sensitizes gastric cancer to cuproptosis and represses immune evasion [J]. Free Radic Biol Med, 2026, 250: 399–410.
30. REN Q, ZHU X, WANG N, et al. MiR-133a-5p Facilitates Cuproptosis in Hepatocellular Carcinoma Through Targeting of ATP7B [J]. J Inflamm Res, 2025, 18: 6607–22.
31. XIANG H, LUO M, HOU P, et al. miR-124-3p combined with miR-506-3p delay hepatic carcinogenesis via modulating sirtuin 1 [J]. Biomarkers, 2021, 26(3): 196–206.
32. MAJID A, WANG J, NAWAZ M, et al. miR-124-3p Suppresses the Invasiveness and Metastasis of Hepatocarcinoma Cells via Targeting CRKL [J]. Front Mol Biosci, 2020, 7: 223.
33. BERTHELOOT D, LATZ E, FRANKLIN B S. Necroptosis, pyroptosis and apoptosis: an intricate game of cell death [J]. Cell Mol Immunol, 2021, 18(5): 1106–21.
34. MOYER A, TANAKA K, CHENG E H. Apoptosis in Cancer Biology and Therapy [J]. Annu Rev Pathol, 2025, 20(1): 303–28.
35. GUO Z, CHEN D, YAO L, et al. The molecular mechanism and therapeutic landscape of copper and cuproptosis in cancer [J]. Signal Transduct Target Ther, 2025, 10(1): 149.

Figures

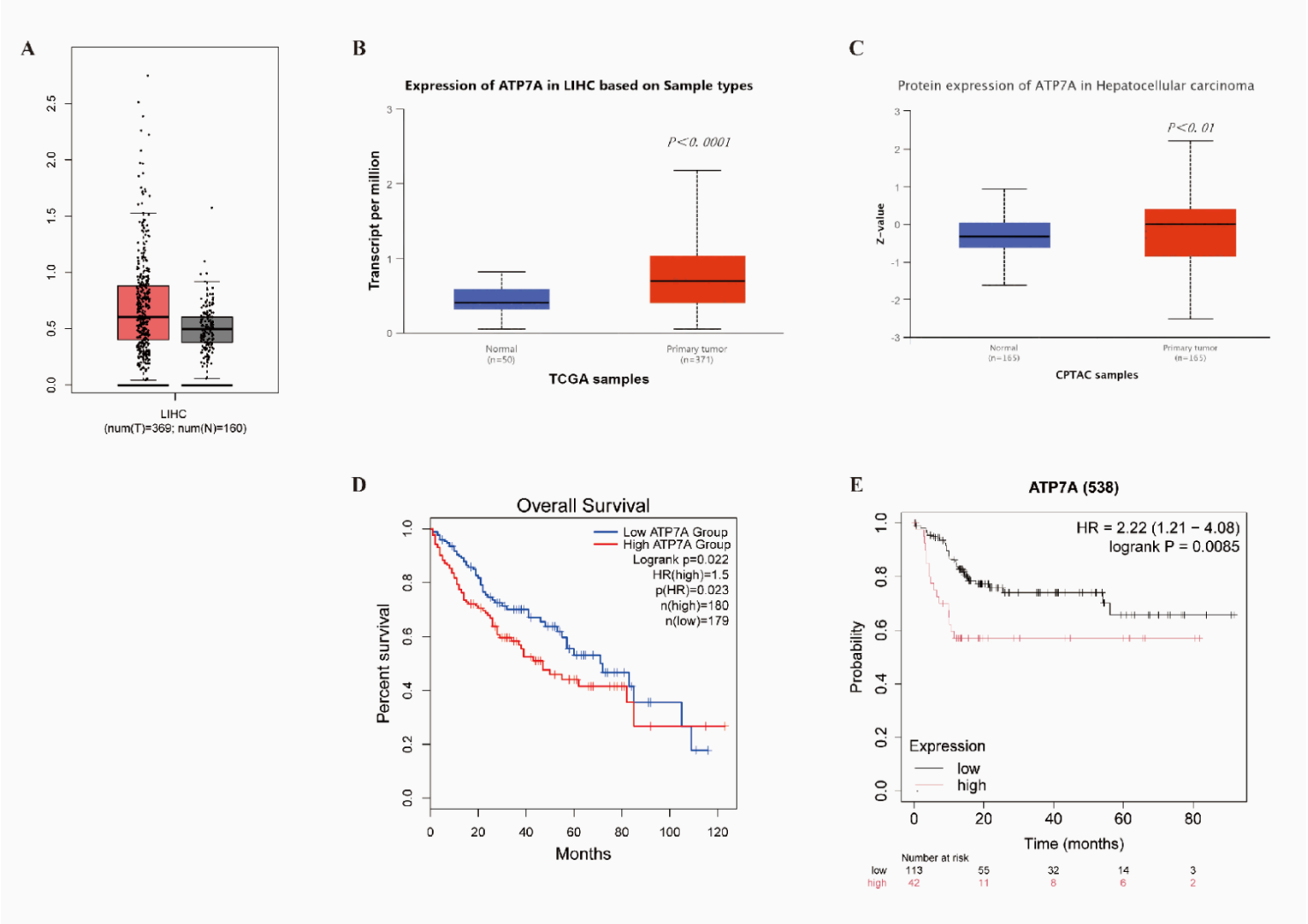


Figure 1

Bioinformatics analysis of ATP7A expression and its prognostic significance in hepatocellular carcinoma

(A) Comparison of ATP7A expression levels between hepatocellular carcinoma (LIHC) tissues and normal liver tissues in the GEPIA 2 dataset; (B) Analysis of ATP7A mRNA expression differences based on TCGA transcriptomic data; (C) Analysis of ATP7A protein expression differences based on CPTAC proteomic data; (D) Kaplan–Meier survival analysis of OS based on the GEPIA 2 database, comparing high and low ATP7A expression groups; (E) Survival analysis based on the Kaplan–Meier Plotter database evaluating the association between ATP7A expression and prognosis in patients with hepatocellular carcinoma.

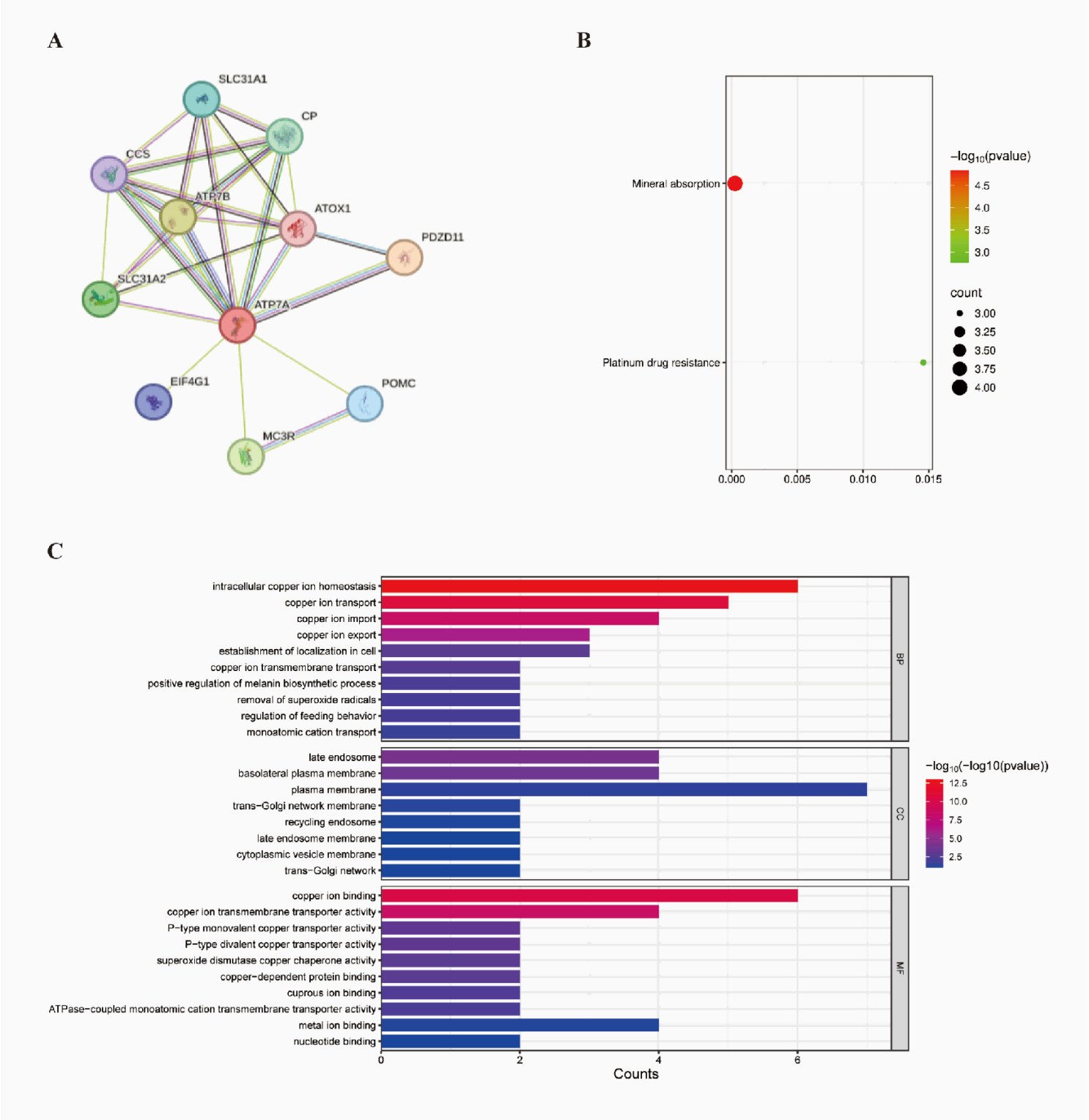
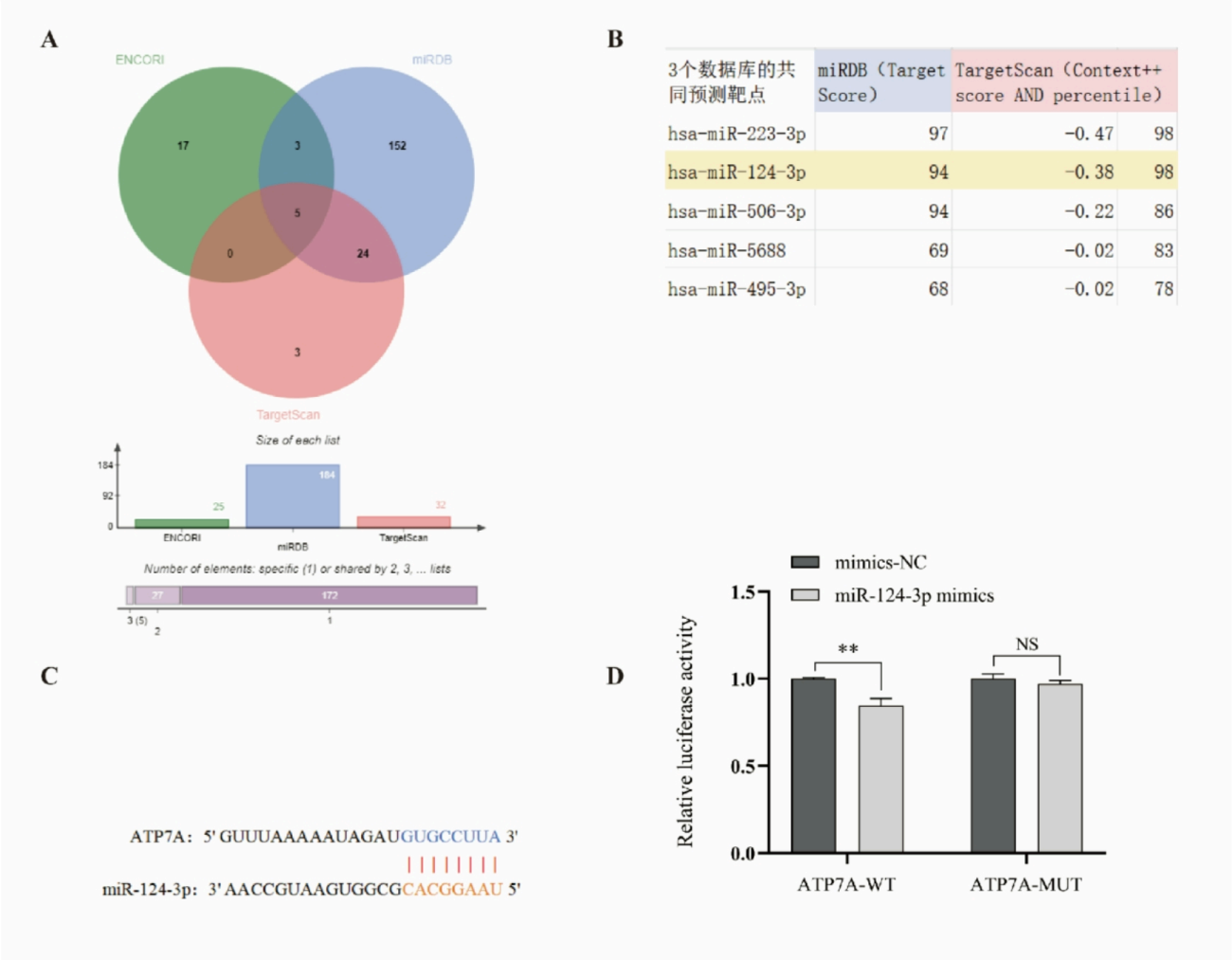


Figure 2

Bioinformatic analysis reveals the potential involvement of ATP7A in copper metabolism-related biological processes

(A) Protein-protein interaction (PPI) network analysis of ATP7A and its interacting proteins based on the STRING database. (B-C) Bioinformatic annotation of ATP7A-associated genes using GO classification

(C) and KEGG pathway enrichment analysis (B),revealing the potential biological processes and signaling pathways involved in ATP7A regulation.



3个数据库的共同预测靶点	miRDB (Target Score)	TargetScan (Context++ score AND percentile)	
hsa-miR-223-3p	97	-0.47	98
hsa-miR-124-3p	94	-0.38	98
hsa-miR-506-3p	94	-0.22	86
hsa-miR-5688	69	-0.02	83
hsa-miR-495-3p	68	-0.02	78

Figure 3

Bioinformatic prediction and experimental validation of the targeting relationship between miR-124-3p and ATP7A

(A) Candidate miRNAs targeting ATP7A were screened using three databases (ENCORI, miRDB, and TargetScan). (B) Summary of prediction scores for candidate miRNAs across the three databases. (C) Predicted binding site and seed sequence pairing between miR-124-3p and the 3'-UTR of ATP7A based on TargetScan analysis. (D) Dual-luciferase reporter assay identifying ATP7A as a direct target of miR-124-3p. Note: NS, not significant; $^{**}P < 0.01$.

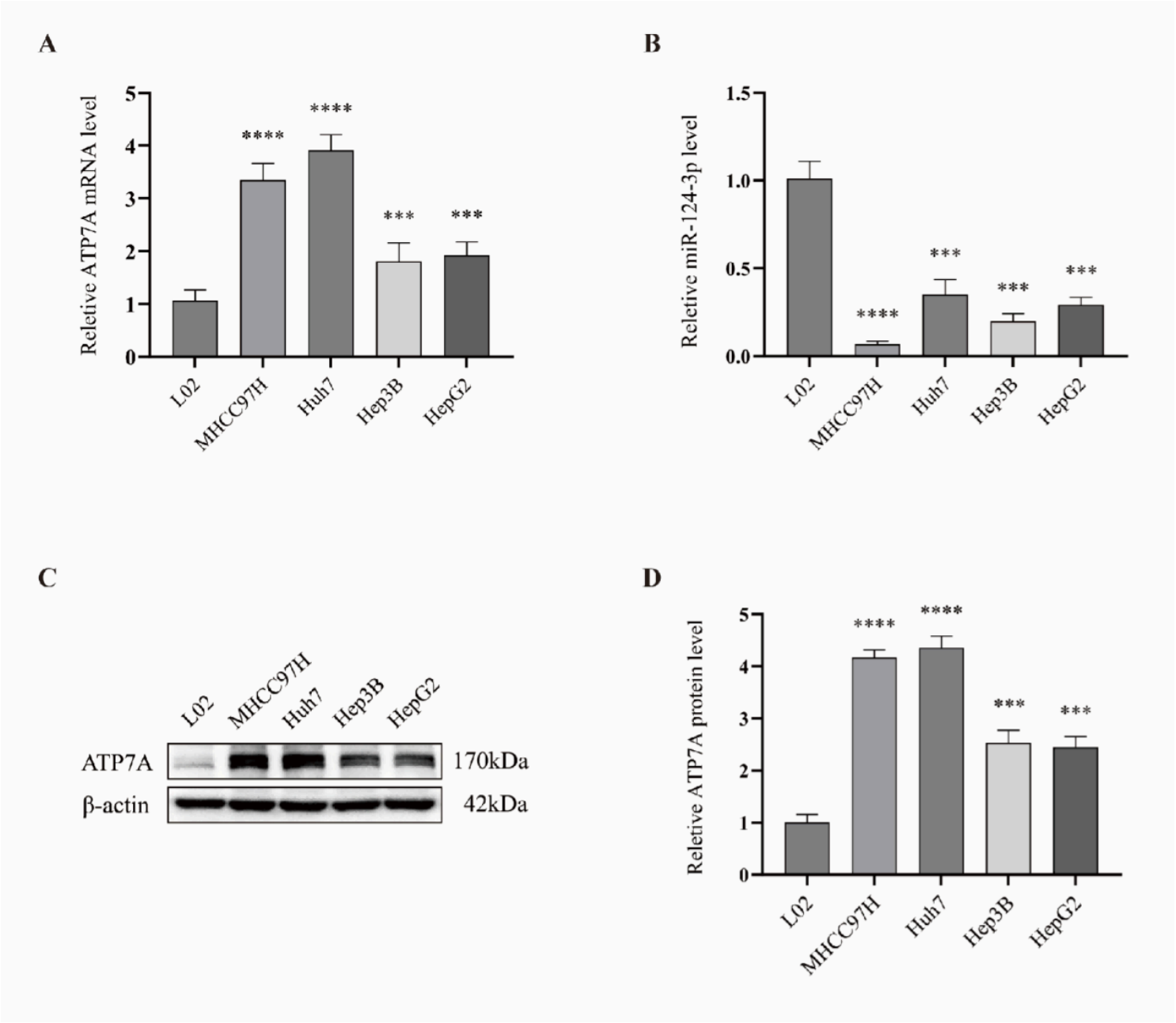


Figure 4

Expression patterns of miR-124-3p and ATP7A in normal hepatocytes and hepatocellular carcinoma cell lines

(A) qRT-PCR analysis of ATP7A mRNA expression in normal hepatocytes (L02) and hepatocellular carcinoma (HCC) cell lines. (B) qRT-PCR analysis of miR-124-3p expression in the indicated cell lines. (C) Representative immunoblotting images showing ATP7A protein levels in normal hepatocytes and HCC cell lines. (D) Relative ATP7A protein abundance was quantified by grayscale analysis.**Note: All statistical comparisons were performed relative to the L02 cell group. ***P< 0.001, ****P□0.0001.

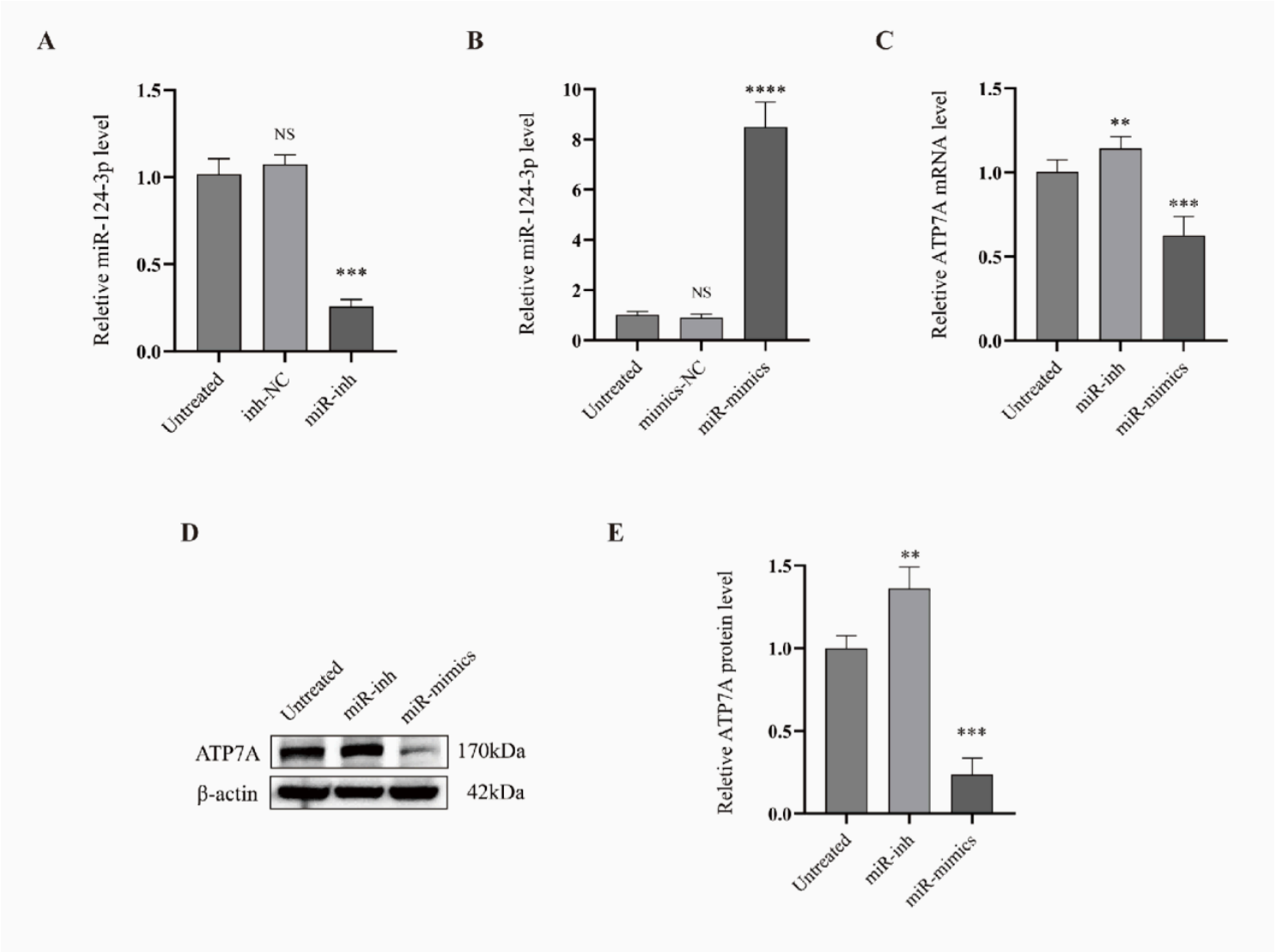


Figure 5

Validation of miR-124-3p-mediated negative regulation of ATP7A expression in MHCC97H cells

(A) Validation of miR-124-3p knockdown efficiency in MHCC97H cells by qRT-PCR. (B) Confirmation of miR-124-3p overexpression in MHCC97H cells using qRT-PCR.(C) qRT-PCR analysis of ATP7A mRNA expression in MHCC97H cells following different treatments. (D) Western blot analysis of ATP7A protein expression in MHCC97H cells. (E) Densitometric quantification of ATP7A protein expression. **Note: Untreated, untreated group; NC, negative control; miR-mimics, miR-124-3p mimics; miR-inh, miR-124-3p inhibitor. All statistical comparisons were performed relative to the Untreated group. NS, not significant; ***P* < 0.01, ****P* < 0.001, *****P* < 0.0001.

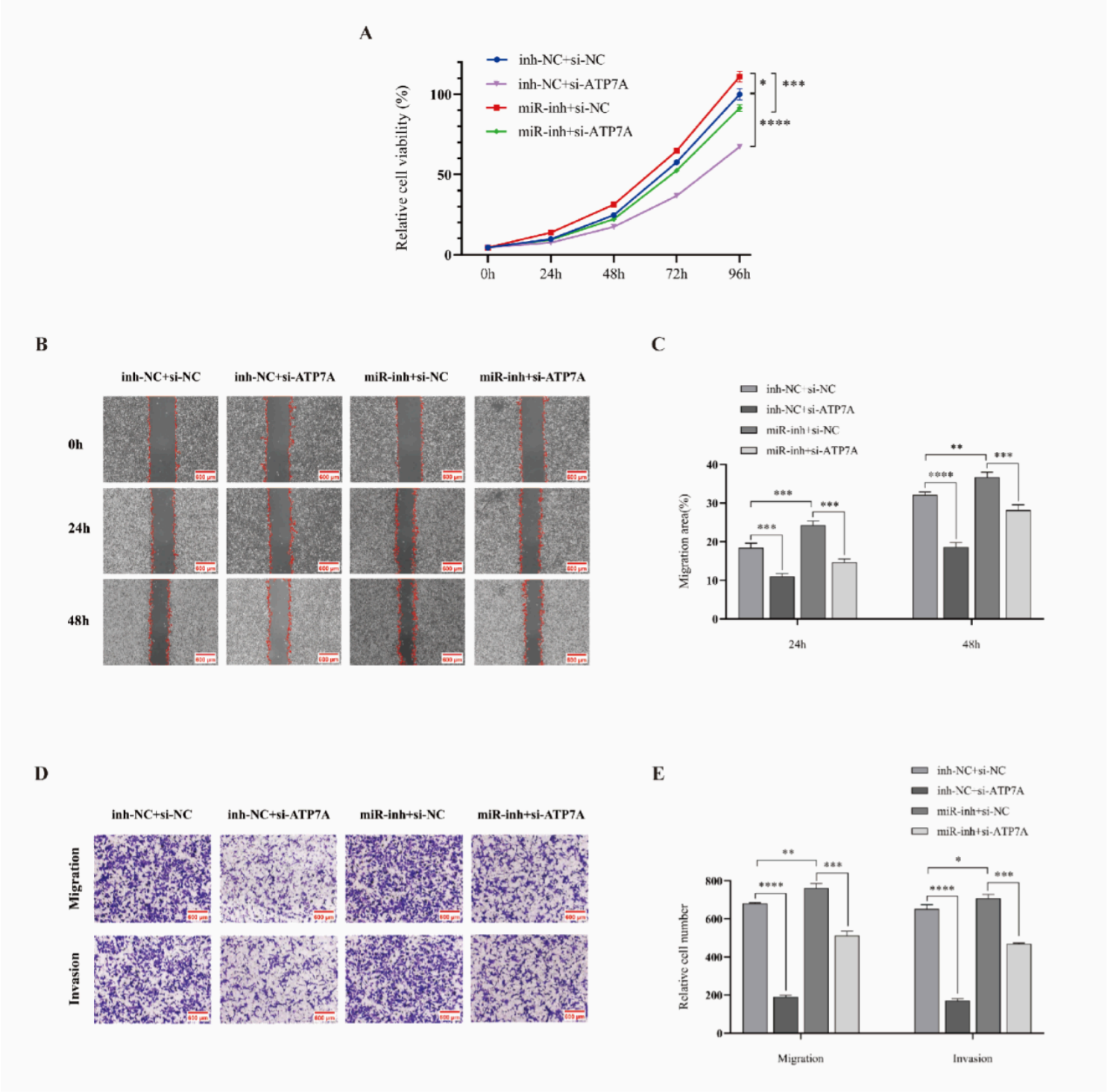


Figure 6

miR-124-3p regulates the proliferation, migration, and invasion of MHCC97H cells by targeting ATP7A

(A) Cell proliferation activity of MHCC97H cells in the indicated groups was assessed by CCK-8 assay at 0, 24, 48, 72, and 96 h after transfection. (B) Representative images of wound healing assays showing the migratory ability of MHCC97H cells at 0, 24, and 48 h. (C) Quantitative analysis of wound closure rates in the indicated groups. (D) Representative crystal violet staining images of Transwell assays evaluating cell migration and invasion abilities. (E) Quantification of migrated and invaded cells in

Transwell assays. Note: si-NC, small interfering RNA negative control; si-ATP7A, ATP7A-specific small interfering RNA. *$P<0.05$ **$P<0.01$ ***$P<0.001$ ****$P<0.0001$

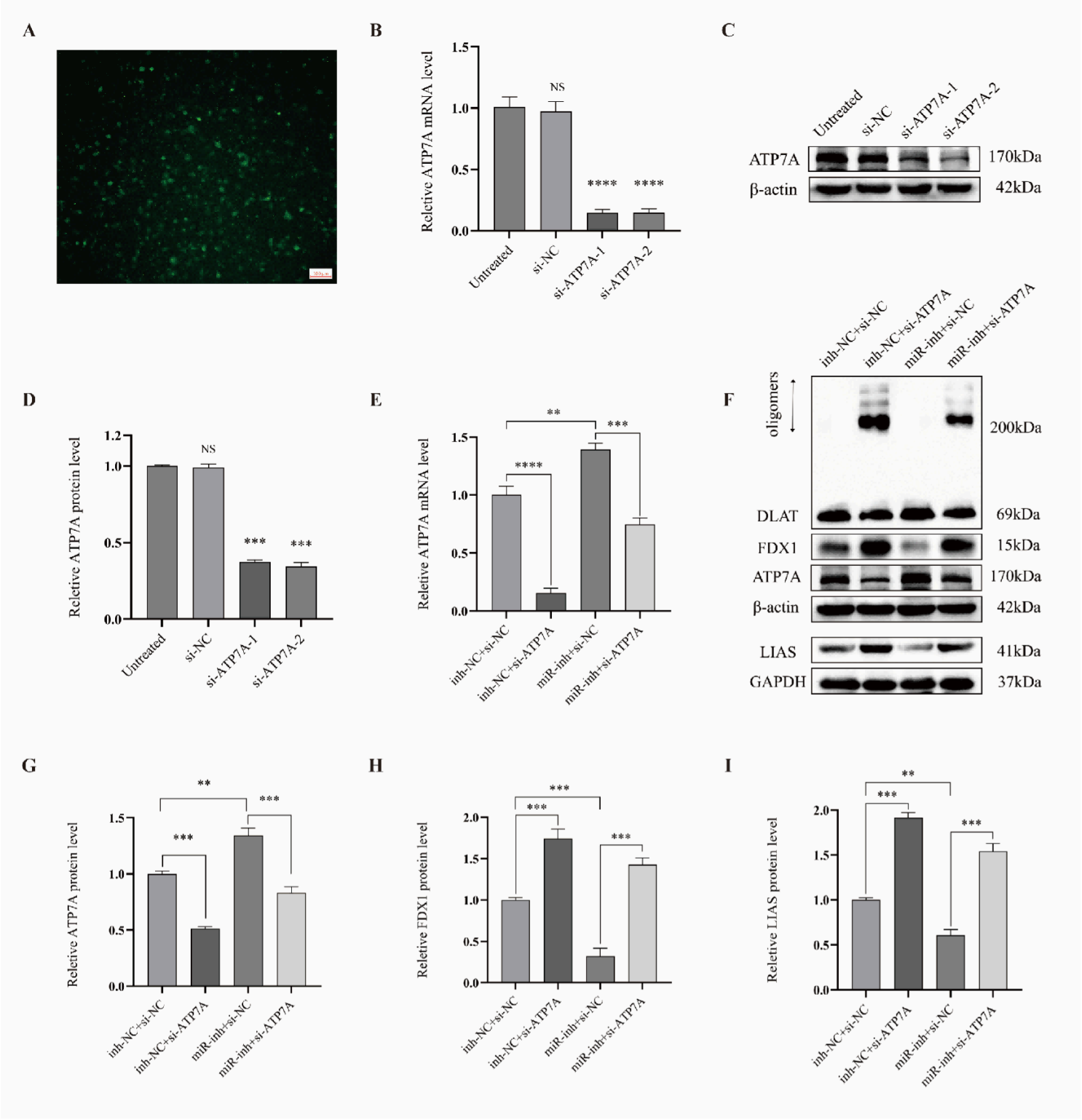


Figure 7

The miR-124-3p/ATP7A axis regulates cuproptosis-associated molecular changes in HCC cells

(A) Visualization of intracellular FAM fluorescence in MHCC97H cells following oligonucleotide transfection.(B) qRT-PCR analysis of ATP7A mRNA expression in MHCC97H cells transfected with different ATP7A siRNAs for screening effective knockdown sequences. (C) Western blot analysis of ATP7A protein expression after ATP7A silencing. (D) Densitometric quantification of ATP7A protein expression. (E) qRT-PCR analysis of ATP7A mRNA expression in the four rescue groups. (F) Western blot analysis of ATP7A, FDX1, and LIAS expression, together with DLAT oligomerization under non-reducing conditions, in the indicated groups. (G-I) Quantitative analysis of ATP7A, FDX1, and LIAS protein expression based on densitometric measurements. **Note: NS, not significant; ***P*0.01***P*0.001 ****P*0.0001.

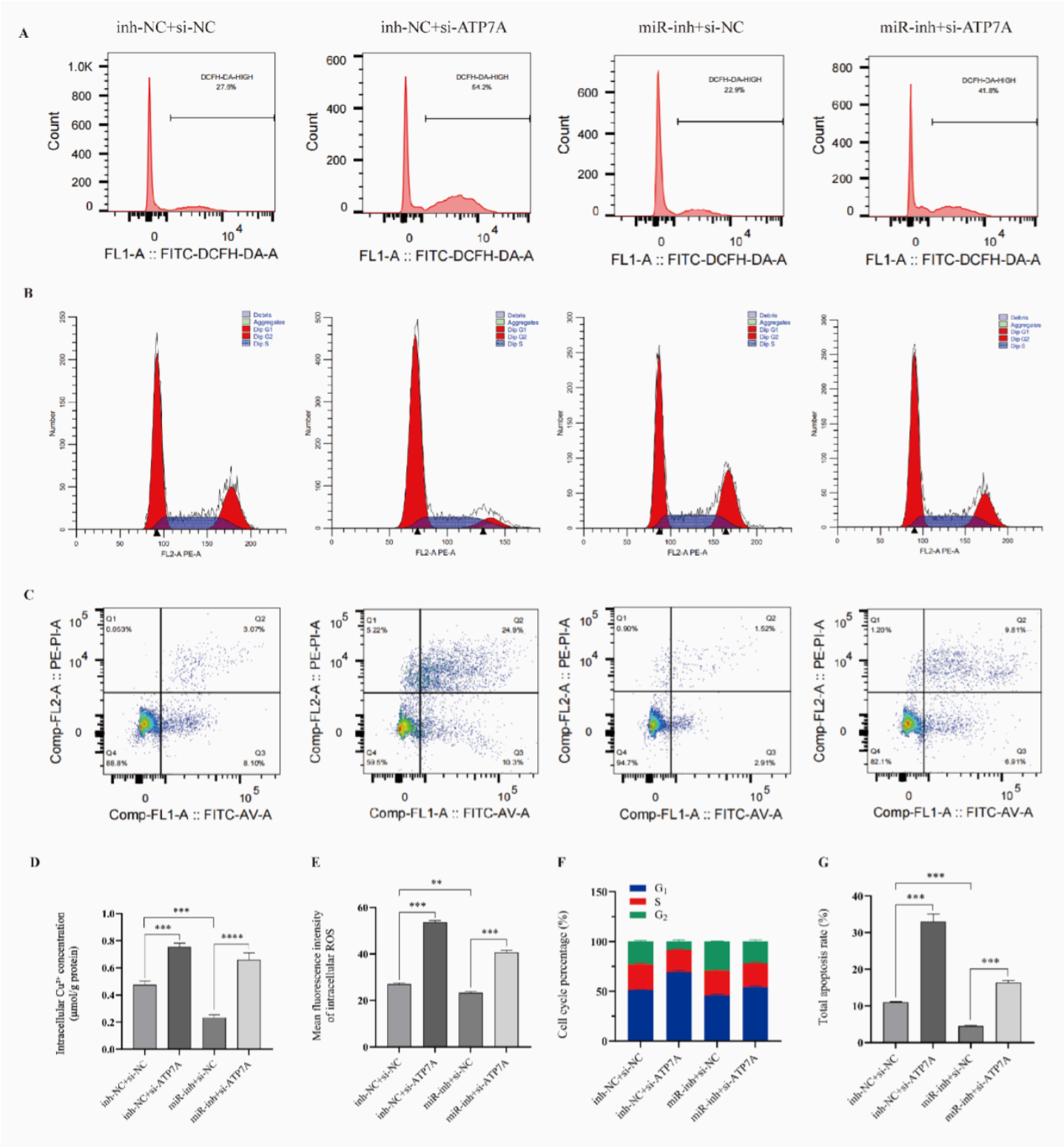


Figure 8

The miR-124-3p/ATP7A axis influences cuproptosis-related phenotypes in HCC cells by regulating copper homeostasis

(A) Representative flow cytometry profiles showing intracellular ROS levels in MHCC97H cells from the indicated groups. (B) Representative flow cytometry profiles showing cell cycle distribution in MHCC97H

cells. (C) Representative Annexin V-FITC/PI staining profiles showing apoptosis in MHCC97H cells. (D) Measurement of intracellular Cu^{2+} levels in MHCC97H cells from the indicated groups. (E) Quantitative analysis of intracellular ROS levels based on mean fluorescence intensity (MFI). (F) Quantitative analysis of cell cycle distribution among G1, S, and G2/M phases. (G) Quantitative analysis of total apoptosis rates. **Note: Intracellular ROS levels were detected using the DCFH-DA probe by flow cytometry. Data are presented as mean ± SD from three independent experiments. **P□0.01□***P□0.001□****P□0.0001.

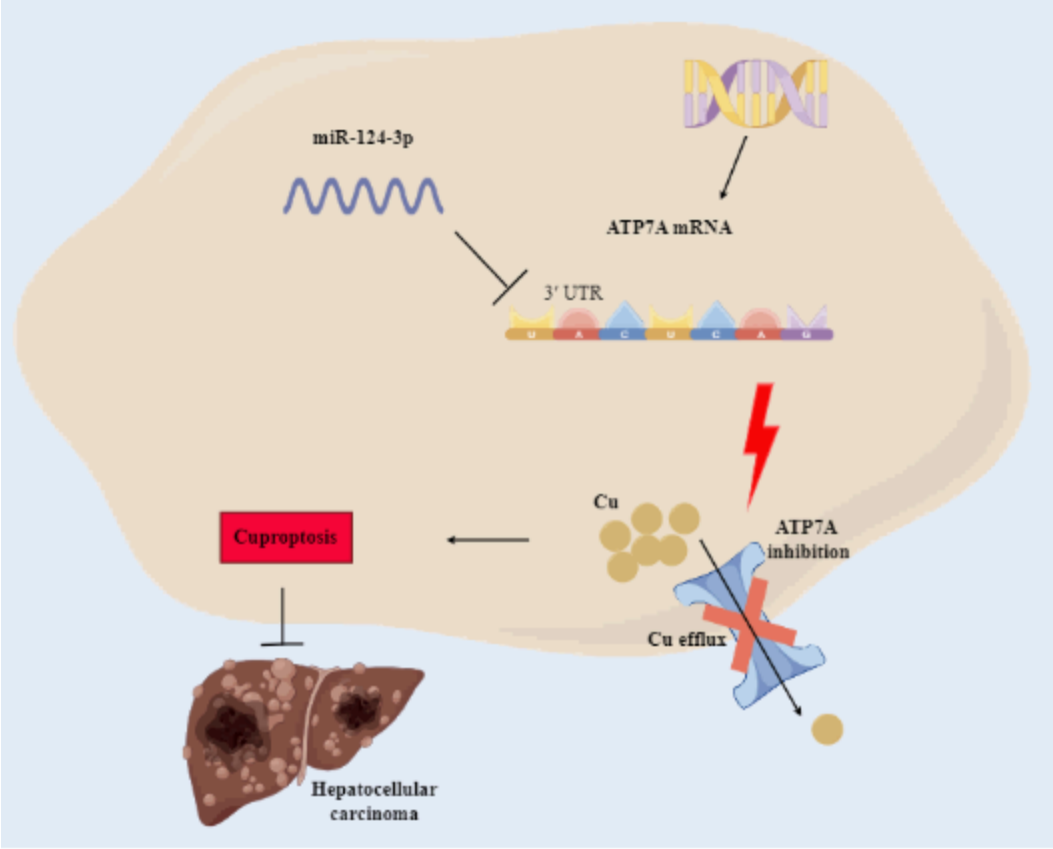


Figure 9

Proposed model illustrating the role of the miR-124-3p/ATP7A axis in regulating copper homeostasis and cuproptosis sensitivity in hepatocellular carcinoma.

Supplementary Files

This is a list of supplementary files associated with this preprint. Click to download.

- ExplanationforWesternblotrawimages.pdf
- PCR.xlsx